

## New insights on the crystalline forms in binary systems of *n*-alkanes: Characterization of the solid ordered phases in the phase diagram tricosane + pentacosane

F. Rajabalee,<sup>a)</sup> V. Métivaud, D. Mondieig, and Y. Haget

Centre de Physique Moléculaire Optique et Hertzienne, UMR 5798 au CNRS Université Bordeaux I, F-33405 Talence Cedex, France

M. A. Cuevas-Diarte

Departament de Cristal·lografia, Universitat de Barcelona, Martí i Franquès, E-08028 Barcelona, Spain

(Received 26 January 1998; accepted 18 February 1999)

X-ray diffraction analyses of the pure components *n*-tricosane and *n*-pentacosane and of their binary mixed samples have enabled us to characterize the crystalline phases observed at “low temperature.” Contrary to what was announced in literature on the structural behavior of mixed samples in odd-odd binary systems with  $\Delta n = 2$ , the three domains are not all orthorhombic. This work has enabled us to show that two of the domains are, in fact, monoclinic ( $Aa$ ,  $Z = 4$ ), and the other one is orthorhombic ( $P_{ca2_1}$ ,  $Z = 4$ ). The conclusions drawn in this work can easily be transposed to other binary systems of *n*-alkanes.

### I. INTRODUCTION

Polymorphism of *n*-alkanes<sup>1–23</sup> ( $C_nH_{2n+2}$ ; hereafter denoted by  $C_n$ ) and determination of binary phase diagrams<sup>22–41</sup> in the alkane family have been reported on in recent years in numerous publications. The polymorphism of *n*-alkanes is rather well known where many solid-solid phase transitions have been observed as a function of temperature.

For the odd alkanes, unitary phase diagrams showing the transition temperatures as a function of chain length (*n*) have been determined<sup>9,10</sup> for the range going from  $C_9$  to  $C_{45}$  where four solid ordered phases (we call ordered phases those which are not accompanied with orientational disorders like the rotator phases) have been identified: two orthorhombic forms (space groups  $P_{cam}$  and  $P_{nam}$ ) and two monoclinic forms (space groups  $Aa$  and  $A2$ ). All four phases possess four molecules per unit cell ( $Z = 4$ ). However, these unitary phase diagrams stress only on the low-temperature region, the rotator domains being given as a set. Five rotator forms are known to exist,<sup>19,20</sup> denoted  $R_I$ ,  $R_{II}$ ,  $R_{III}$ ,  $R_{IV}$ , and  $R_V$ , and are observed until  $C_{39}H_{80}$ . In the range  $8 \leq n \leq 28$ , Roblès *et al.*<sup>1,22</sup> and Espeau *et al.*<sup>2</sup> give the complete phase transitions in these alkanes incorporating the rotator forms. Odd alkanes always show at least one rotator phase before melting.

For the even alkanes, the polymorphism is even more complex and the polymorphic behavior is often different, depending on the initial state of the alkane.

A triclinic form  $T_p$  ( $P\bar{1}$ ,  $Z = 1^3$ ) is observed in the range  $8 \leq n \leq 24$ ,<sup>1,2,22</sup> while several monoclinic modifications  $M_{011}$ ,  $M_{201}$ ,  $M_{012}$ , and  $M_{101}$  are found in longer even alkanes as from  $C_{26}$ .<sup>23</sup> All these forms have the same space group<sup>4–6,23</sup> ( $P_{2_1/a}$ ,  $Z = 2$ ) but differ by the shift of adjacent molecules in the planes ( $b^*c$  for  $M_{011}$  and  $M_{012}$  and  $a^*c$  for  $M_{201}$  and  $M_{101}$ ) of a whole number of  $CH_2$  units. In the  $M_{hkl}$  notation, the (*hkl*) describes the plane formed by the methyl end groups ( $CH_3$ ) in the referential of the orthorhombic subcell. Two orthorhombic forms are observed:  $O_p$  ( $P_{ca2_1}$ ,  $Z = 4^7$ ) and  $O_{II}$  ( $P_{bcn}$ ,  $Z = 4$  or  $P_{bca}$ ,  $Z = 4^8$ ). The latter is observed only in  $C_{36}H_{74}$ ,<sup>8,23</sup> which results from an alternative stacking of molecular layers of type  $M_{011}$  and  $M_{0\bar{1}1}$ .<sup>6</sup> Several of these forms are metastable (for example,  $O_p$  which is involved in the binary phase diagram given in this paper). New phases have been identified as triclinic ( $T_{111}$  in  $C_{46}$  and  $T_{212}$  in  $C_{44}$ ,  $C_{46}$ , and  $C_{50}$ ) which are described as the result of two shifts (the  $M_{101}$  one followed by the  $M_{011}$  shift for  $T_{111}$  and the  $M_{101}$  shift followed by the  $M_{012}$  one for  $T_{212}$ ).<sup>23</sup> Unlike odd alkanes, rotator phases appear only as from  $C_{22}H_{46}$ .<sup>1,2,22</sup>

The study of binary phase diagrams (temperature versus composition) has revealed a complex structural behavior of the mixed samples<sup>28–41</sup> where other forms than those seen in the components are observed and which are stabilized by mixing. The earliest binary phase diagram showing multiple one-phase domains at low temperature (temperature domain where the ordered phases are observed) is that of Lüth *et al.*<sup>28</sup> for the system  $C_{20}$ – $C_{22}$ . A single crystal of the mixed sample  $C_{20}(0.75)C_{22}(0.25)$  was analyzed and a space group was proposed ( $B_{b2_1m}$ ). Smith<sup>30</sup> carried out single crystal

<sup>a)</sup>Address all correspondence to this author.  
e-mail: frajabal@frbdx11.cribx1.u-bordeaux.fr

measurements on two mixed samples of composition ratios 1 : 1 and 2 : 1 in the C<sub>24</sub>–C<sub>26</sub> system. He supposed that both mixed samples were orthorhombic  $P_{nam}$  with  $Z = 8$  for the 1 : 1 sample and  $Z = 12$  for the 2 : 1 sample. Moreover, he pointed out that single crystal data were obtained for 1 : 1 and 2 : 1 composition ratios for the C<sub>23</sub>–C<sub>25</sub>, C<sub>24</sub>–C<sub>27</sub>, C<sub>28</sub>–C<sub>30</sub>, and C<sub>23</sub>–C<sub>24</sub> systems and that the packing arrangement is the same as that found for the C<sub>24</sub>–C<sub>26</sub>. More recently, Gerson and Nyburg<sup>29</sup> working on the mixed sample C<sub>24</sub>(0.77)C<sub>26</sub>(0.23) proposed the same space group as Lüth *et al.* However, no phase diagram of the C<sub>24</sub>–C<sub>26</sub> system was given and the samples studied by these authors surprisingly correspond to two phase regions.<sup>31,38</sup> Moreover, Achour-Boudjema *et al.*,<sup>31</sup> working on 24 mixed samples of the above system and in particular, on the diffraction pattern of the mixed sample studied by Gerson and Nyburg,<sup>29</sup> could not index all the diffraction lines on the basis of the  $B_{b2,m}$  structure.

To our knowledge, the first work on the binary system C<sub>23</sub>–C<sub>25</sub> (which is the subject of this paper) is that of Retief *et al.*<sup>42</sup> Their phase diagram was very simple but not correct since the polymorphism of the components C<sub>23</sub> and C<sub>25</sub> was not well defined. A complete miscibility both at high and low temperature was proposed. Complex structural behavior of the mixed samples in this system was recently observed by Jouti *et al.*<sup>34,35</sup> At room temperature, these authors have shown the existence of seven one-phase regions in the binary system and they supposed that all the phases are orthorhombic and are denoted by them as  $\beta 0(C_{23})$ ,  $\beta' 0(C_{23})$ ,  $\beta'' 1$ ,  $\beta' 1$ ,  $\beta'' 2$ ,  $\beta' 0(C_{25})$ ,  $\beta 0(C_{25})$ . The two couples  $\beta 0$  and  $\beta' 0$  come from the polymorphism of the components C<sub>23</sub> and C<sub>25</sub> while the three other forms  $\beta'' 1$ ,  $\beta' 1$ , and  $\beta'' 2$  are observed only in the mixed samples. However, no space group has been assigned to these forms and no possible explanation was given which could explain why these forms are observed in the mixed samples. The present work done within the REALM (a European association for the study of molecular alloys) forms part of a global research project on syncrystallization between components belonging to families of molecular substances.

The paper based on the binary system C<sub>23</sub> + C<sub>25</sub> reports new findings on these crystalline forms. Indeed, experimental results on this system and on other binary systems and, in particular, on C<sub>26</sub> + C<sub>28</sub> (the subject of another paper) have enabled us to characterize for the first time the three intermediate forms and to propose, therefore, a new phase diagram for the binary system C<sub>23</sub>–C<sub>25</sub>. The scope of this work is even wider since these phases are also observed in other binary systems<sup>31–41</sup> of *n*-alkanes [with a chain-length difference ( $\Delta n$ ) equal to 1 or 2]. In other words, this paper leads to a complete characterization of all solid ordered

forms observed in all binary systems of *n*-alkanes (the components belonging to the range C<sub>16</sub> to C<sub>28</sub>).

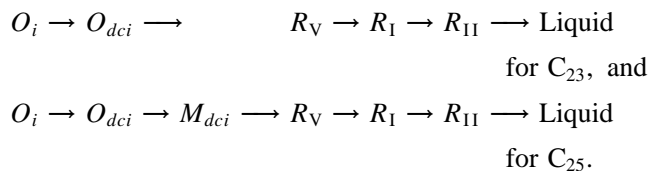
## II. EXPERIMENTAL

Tricosane and pentacosane were purchased from Fluka and Aldrich, respectively. Their purity grades are 99.3% for C<sub>23</sub> and 99.1% for C<sub>25</sub> as determined by gas chromatography and mass spectrometry analyses. Binary mixed samples were prepared according to the “melting-quenching” method: the components are weighted, melted together, mixed thoroughly to obtain an entirely homogeneous sample, and finally quenched into liquid nitrogen.

Calorimetric measurements were performed using a Perkin-Elmer DSC7 operating in the liquid nitrogen subambient mode. Differential scanning calorimetry (DSC) runs were carried out on 4 mg samples, at a heating rate of 2 K min<sup>-1</sup>. The calibration was made with substances of known transition temperatures and enthalpies (water, naphthalene, and indium). The different characteristic temperatures were determined from the DSC curves by using the shape factor method.<sup>43,44</sup> The random part of the uncertainties is estimated using the student’s method with a 95% threshold of reliability. A minimum of four independent experiments were carried out for each composition. X-ray diffraction patterns were recorded in the range  $4^\circ \leq 2\theta \leq 60^\circ$  using a Siemens D500 vertical powder diffractometer which works in the reflection mode with Cu K $\alpha_1$  radiation ( $\lambda = 0.15406$  nm). The *n*-alkanes and their mixed samples are known to have a weak x-ray absorption coefficient and, therefore, to avoid the diffraction lines of copper and nickel due to the sample holder which disturbs the analyses of the diffractograms, a very thin plate of glass was placed between the sample to analyze and the holder. All data were collected with a 0.04° 2 $\theta$  steps and 5 s interval time.

## III. PURE COMPONENT PROPERTIES

The polymorphism of C<sub>23</sub> and C<sub>25</sub> has already been studied<sup>1,22</sup> in the REALM and is as follows:



Low-temperature phases      High-temperature phases

The subscript *dci* stands for “*d*éfauts de *c*onformation dans les alcanes *i*mpairs,” the French words for conformational defects in the odd alkanes. The two orthorhombic forms  $O_i$  and  $O_{dci}$  and the monoclinic  $M_{dci}$  form are

observed only in odd alkanes which explains the use of the subscript *i* (for “impair,” French word for odd). The  $O_{dci}$  and  $M_{dci}$  forms are observed mainly due to end-gauche defects<sup>9,21,39</sup> and justifying the subscript *dc*. In the mixed samples, we will see later that a new form is observed denoted by  $O_p$ . This form is orthorhombic and, in pure alkanes, this phase is metastable and observed only in even forms.<sup>23</sup> The subscript *p* therefore stands for “pair,” the French word for even.

Single crystal of sufficient dimension was obtained for  $C_{23}$  by Smith<sup>45</sup> who identified the  $O_i$  phase as orthorhombic (space group  $P_{cam}$ ,  $Z = 4$ ) and allotted the same space group to the other odd alkanes  $C_{21}$  to  $C_{29}$ . It is now known that the  $O_i$  phase is observed in all odd alkanes<sup>1,2,18,21,22</sup> at least until  $C_{45}H_{92}$ . The cell parameters measured at  $T = 291$  K for both components<sup>1,22</sup> are  $a = 0.7467(8)$  nm,  $b = 0.4983(7)$  nm, and  $c = 6.219(4)$  nm for  $C_{23}$  and  $a = 0.7449(10)$  nm,  $b = 0.4968(5)$  nm, and  $c = 6.726(7)$  nm for  $C_{25}$ .

The  $O_{dci}$  phase was first observed by Snyder *et al.*<sup>9</sup> who detected a low energetic transition  $O_i \rightarrow O_{dci}$  in  $C_{25}$ ,  $C_{27}$ , and  $C_{29}$  and noted this transition as the  $\delta$ -transition without proposing a space group for this phase. The latter was also observed in  $C_{23}$ .<sup>15</sup> This form is not observed as from  $C_{29}$ .<sup>9,46,47</sup> However, from the unitary phase diagram presented by Urabe and Takamizawa<sup>10</sup> and reproduced by Nozaki *et al.*,<sup>48</sup> the  $O_{dci}$  form is observed till  $C_{39}$ . It seemed that Urabe and Takamizawa<sup>10</sup> have worked with highly pure samples, but this was also the case of Piesczek *et al.*<sup>46</sup> The contradiction of Urabe's findings with those of Snyder *et al.*<sup>9</sup> and Piesczek *et al.*<sup>46</sup> is still not clear. The space group of the  $O_{dci}$  phase was determined by Nozaki *et al.*<sup>21</sup> by x-ray powder diffraction using the Rietveld profile refinement method and later confirmed by our work.<sup>39</sup>  $O_{dci}$  is orthorhombic (space group  $P_{nam}$ ,  $Z = 4$ ). The cell parameters of  $C_{23}$  measured at  $T = 312$  K<sup>1,22</sup> are  $a = 0.7546(8)$  nm,  $b = 0.4989(7)$  nm, and  $c = 6.226(4)$  nm and those of  $C_{25}$  at 317 K<sup>1</sup> are  $a = 0.7552(10)$  nm,  $b = 0.4980(5)$  nm, and  $c = 6.733(7)$  nm.

The  $M_{dci}$  form was first observed and identified by Piesczek and co-workers<sup>46,47</sup> on the alkane  $C_{33}$  from single crystal data analysis. They show that the symmetry is monoclinic (space group  $Aa$ ,  $Z = 4$ ) and that the subcell is orthorhombic. This phase has been observed in all the odd alkanes with  $25 \leq n \leq 45$ .<sup>9,10</sup> The cell parameters measured at  $T = 319$  K<sup>1,22</sup> are  $a = 0.7553$  nm,  $b = 0.4993$  nm,  $c = 6.753$  nm, and  $\beta = 91.54$ . Jouti *et al.*<sup>34,35</sup> who worked, like us, with the  $C_{25}$  purchased from Aldrich with the same stated purity did not detect this phase.

Differentiating among the diffraction patterns of the solid ordered phases  $O_i$ ,  $O_{dci}$ , and  $M_{dci}$  is necessary in order to characterize the forms observed in the mixed samples of the binary system  $C_{23}$ – $C_{25}$ . Since the three

above forms are observed in  $C_{25}$  with increasing temperature, accurate x-ray analysis of this component is therefore of great interest.

X-ray diffraction patterns of the  $O_i$ ,  $O_{dci}$ , and  $M_{dci}$  forms of  $C_{25}$  were recorded at 293, 318, and 320 K, respectively. The cell parameters for the three phases are the following:

$$\begin{aligned} \text{Form } O_i : \quad & a = 0.7461(2) \text{ nm} \quad b = 0.4987(4) \text{ nm} \\ & \quad \quad \quad \quad \quad \quad \quad \quad c = 6.7317(10) \text{ nm} \\ \text{Form } O_{dci} : \quad & a = 0.7563(1) \text{ nm} \quad b = 0.4993(1) \text{ nm} \\ & \quad \quad \quad \quad \quad \quad \quad \quad c = 6.7438(11) \text{ nm} \\ \text{Form } M_{dci} : \quad & a = 0.7573(4) \text{ nm} \quad b = 0.5011(3) \text{ nm} \\ & \quad \quad \quad \quad \quad \quad \quad \quad c = 6.7631(9) \text{ nm} \quad \beta = 91.64(4)^\circ \end{aligned}$$

These values are in agreement with those of Roblès *et al.*<sup>1,22</sup>

The phase changes  $O_i \rightarrow O_{dci} \rightarrow M_{dci}$  are accompanied with relatively low enthalpy effects with regard to the  $M_{dci} \rightarrow R_1$  and the melting enthalpies. The long *c*-parameter and the similarity in symmetries (the monoclinic  $M_{dci}$  form is very close in symmetry to the orthorhombic one of the  $O_i$  and  $O_{dci}$  forms) lead to similar diffraction patterns at low angles ( $2\theta \leq 34^\circ$ ).<sup>21,39</sup> As a result, the diffraction data are shown in this paper only in the pertinent range  $34^\circ \leq 2\theta \leq 60^\circ$ . One of the major problems encountered with the normal alkanes is to index unambiguously the peaks of a powdered diffraction pattern.<sup>28,29</sup> Indeed, the long *c*-parameter (compared to the *a* and *b* ones) results in several possible indexing for a single reflection. This effect is even more pronounced at high angles and specially, as said above, in the range ( $2\theta \geq 34^\circ$ ) sensitive to the phase changes [ $O_i$ ,  $O_{dci}$ ,  $M_{dci}$ , and  $O_p$  (see further on) forms]. Fractional coordinates of the carbon atoms are known only for  $C_{23}$ ,<sup>45</sup> but extrapolation for the other members of the series can be undertaken considering that *a*- and *b*-parameters are identical for the odd alkanes.<sup>1,2,39,45</sup> Therefore, the derivation of atomic coordinates for any other member could be easily derived from the fractional coordinates of the carbon atoms  $C_{(1)}$  and  $C_{(2)}$  of the alkane  $C_{23}$ .<sup>49</sup> We have therefore derived the fractional coordinates of  $C_{25}$  in the  $O_i$  form and obtained the list of reflections with their intensities. The experimental diffraction pattern of the  $O_i$  phase of  $C_{25}$  (see Fig. 1) is indexed using the reflections with the highest intensities. These indexings are in good agreement with those proposed by Nozaki *et al.*<sup>21</sup> and Jouti *et al.*<sup>34</sup> The indexing of the peaks of the  $O_{dci}$  form is based on that of the  $O_i$  form and on the space group  $P_{nam}$  proposed by Nozaki and co-workers.<sup>21</sup> The peaks which are at nearly the same diffraction angle in the  $O_i$  and  $O_{dci}$  forms (changes are due to thermal agitation) are indexed with the same *hkl*. The indexing of the  $M_{dci}$  form is based on that of the  $O_{dci}$  form and

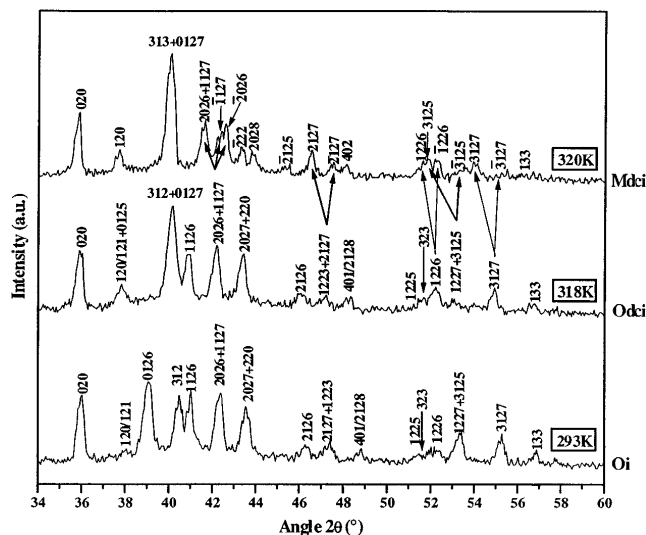


FIG. 1. X-ray diffraction patterns of the  $O_i$ ,  $O_{dci}$ , and  $M_{dci}$  forms of  $C_{25}$  in the range  $34^\circ \leq 2\theta \leq 60^\circ$  recorded at  $T = 293, 318,$  and  $320$  K, respectively.

on the property of the monoclinic symmetry, resulting in a split of the diffraction lines.

The transition  $O_i \rightarrow O_{dci}$  in  $C_{25}$  is mainly characterized by (i) the disappearance of the  $0\ 1\ 26$  at  $2\theta \approx 39^\circ$  in agreement with the extinction conditions imposed by the  $P_{nam}$  space group; (ii) the appearance of the  $0\ 1\ 25$  and  $0\ 1\ 27$  reflections at  $2\theta \approx 38.1^\circ$  and  $2\theta \approx 40.5^\circ$ , respectively. These reflections which are not allowed in the  $O_i$  form ( $P_{cam}$ ) are superposed with the  $1\ 2\ 0/1\ 2\ 1$  and  $3\ 1\ 2$  lines, respectively, and account for the increase of the intensity of the peaks; (iii) the increase in intensity of the  $1\ 2\ 26$  reflection at  $2\theta \approx 52.5^\circ$ ; (iv) the decrease in intensity of the  $1\ 1\ 26$  at  $2\theta \approx 41.2^\circ$ ,  $1\ 2\ 23$  at  $2\theta \approx 47.2^\circ$ , and  $1\ 2\ 27$  reflections at  $2\theta \approx 53.5^\circ$ . The decrease in intensity of these diffraction lines can be explained by the fact that they disappear in the  $M_{dci}$  form which succeeds. On this basis, it seems that the  $O_{dci}$  form is a precursor to the  $M_{dci}$  form.

A consequent shift of the  $hkl$  ( $l = 0, 1, 2, 3$ ) lines toward low angles is observed while those with high  $l$  indices do not show a profound  $2\theta$  displacement (Fig. 1). The rise in temperature leads to an appreciable lateral expansion along the  $a$ -direction (see cell parameters of  $C_{25}$  in the  $O_i$  and  $O_{dci}$  forms) while the expansion along the molecular axis ( $c$ -direction) is not as consequent due to the long  $c$ -parameter. However, discontinuity in the interlayer spacing at each phase transition was observed in  $C_{25}$  and  $C_{27}$ .<sup>39</sup>

The transition  $O_{dci} \rightarrow M_{dci}$  is mainly characterized by (i) the disappearance of the  $1\ 1\ 26, 2\ 1\ 26, 1\ 2\ 25,$  and  $1\ 2\ 27$  reflections at  $2\theta \approx 41^\circ, 2\theta \approx 46^\circ, 2\theta \approx 51.5^\circ,$  and  $2\theta \approx 53^\circ$ , respectively; (ii) the “splitting” of the following reflections located at  $2\theta \approx 42.5^\circ$  ( $2\ 0\ 26$  and

$1\ 1\ 27$ ),  $2\theta \approx 47^\circ$  ( $2\ 1\ 27$ ),  $2\theta \approx 52^\circ$  ( $1\ 2\ 26$ ),  $2\theta \approx 53^\circ$  ( $3\ 1\ 25$ ), and  $2\theta \approx 55^\circ$  ( $3\ 1\ 27$ ).

The reflection conditions imposed by the space group  $Aa$  of the  $M_{dci}$  form are reflected by the disappearance of the diffraction lines  $1\ 1\ 26, 2\ 1\ 26, 1\ 2\ 25,$  and  $1\ 2\ 27$ . Due to the monoclinic symmetry of the  $M_{dci}$  form, each permitted line is “split” into two (as shown by the two arrows drawn in Fig. 1), those having Miller indices with a large  $l$  value are more visible since they are more separated in the high  $2\theta$  range.

The diffraction patterns of all odd alkanes in the  $O_i$  form show a peak located at  $2\theta \approx 39^\circ$ . While the peak is indexed as  $0\ 1\ 26$  in  $C_{25}$ , it is indexed as  $0\ 1\ 24$  in  $C_{23}$ ,  $0\ 1\ 22$  in  $C_{21}$ ,  $0\ 1\ 28$  in  $C_{27}$  and so on, depending on the number of carbon atoms.<sup>39</sup> This is also the case for the other  $hkl$  lines with  $l$  ( $l = n + i, i = 0, 1,$  or  $2$ ).<sup>39</sup> The  $O_{dci}$  and  $M_{dci}$  forms have the same property, that is, peaks at nearly equal angular positions but whose indexing also depend on the number of carbon. This property (independently of the binary system involved, that is of chain length) of odd alkanes is very useful to identify the intermediate phases in binary systems of normal alkanes. Indeed, by simply comparing the powdered diffraction patterns of a sample whose space group is known with that of another sample enables proposing a space group for the latter.

This work being centered on “low temperature” phases, details about the rotator phases in  $C_{23}$  and  $C_{25}$  are given elsewhere.<sup>1,15,16,22</sup>

#### IV. EXPERIMENTAL PHASE DIAGRAM OF $C_{23} + C_{25}$

The experimental phase diagram determined by x-ray diffraction and calorimetric analyses of 19 compositions is given in Fig. 2 where  $x$  denotes the mole fraction in  $C_{25}$ . The symbols  $\blacksquare, \blacklozenge, \blacklozenge,$  and  $\square$  correspond to the  $O_i, O_{dci}, M_{dci},$  and  $O_p$  forms respectively, and their positions in the phase diagram indicate at which temperature levels x-ray analyses were made. The same symbols are used for the diffractograms to point out some reflections specific of one phase which are not present in the other phases.

The phase diagram exhibits no less than seven solid ordered phases, three rotator forms, and three invariants, which are a eutectoid, a peritectoid, and a metatectoid. More details on the determination of this diagram as well as experimental data (temperatures and enthalpies of transition) and thermodynamic analyses of the different equilibria (not the purpose of this paper) will be reported in a further paper. Nevertheless, we can say that the general aspect of our phase diagram is somewhat different from that of Jouti *et al.*<sup>35</sup> For example, these authors proposed a peritectoid invariant

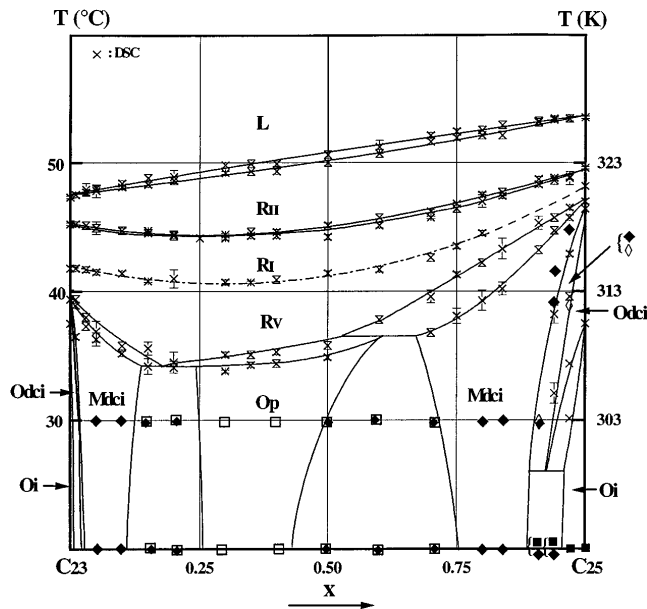


FIG. 2. Phase diagram of the binary system  $C_{23}H_{48}-C_{25}H_{52}$ .

near  $C_{25}$  due to the fact that they did not observe the  $\beta''2$  form (our  $M_{dci}$  form) for the component  $C_{25}$ .

### V. CHARACTERIZATION OF THE (INTERMEDIATE) LOW TEMPERATURE FORMS

The aim of this paper (as we already said) is to characterize the solid ordered phases, that is, the low temperature forms and more particularly the intermediate ones. For that, we have selected only the most pertinent x-ray experiments in order to establish the following main results:

#### A. The one-phase domain denoted $\beta''2$ by Jouti *et al.* comes from the $M_{dci}$ form of $C_{25}$ and therefore is not orthorhombic

These results are clearly testified in Fig. 3 where the x-ray diffraction patterns performed with increasing temperature for molar compositions  $x = 0.97$  and  $x = 0.91$  [Figs. 3(b) and 3(c), respectively] together with the diffractogram of  $C_{25}$  [Fig. 3(a)] (at  $T = 320$  K) are given. In all three cases, the upper form is  $M_{dci}$ . As for the component  $C_{25}$ , the  $O_{dci} \rightarrow M_{dci}$  transition in the mixed sample  $x = 0.97$  [Fig. 3(b)] is mainly characterized by the splitting of the two reflections  $1\ 1\ 27$  and  $2\ 0\ 26$  (see arrows), while the diffraction line  $1\ 1\ 26$  at  $2\theta \approx 41^\circ$  disappears [see, for example, Fig. 3(b)].

#### B. Existence of a metatectoid invariant

For  $x = 0.97$ , starting from 293 K, the observed sequence of domains with increasing temperature [Fig. 3(b)] is  $[O_i] \rightarrow [O_i + O_{dci}] \rightarrow [O_{dci}] \rightarrow [O_{dci} + M_{dci}] \rightarrow [M_{dci}]$ . As for the component  $C_{25}$ , the  $O_i \rightarrow$

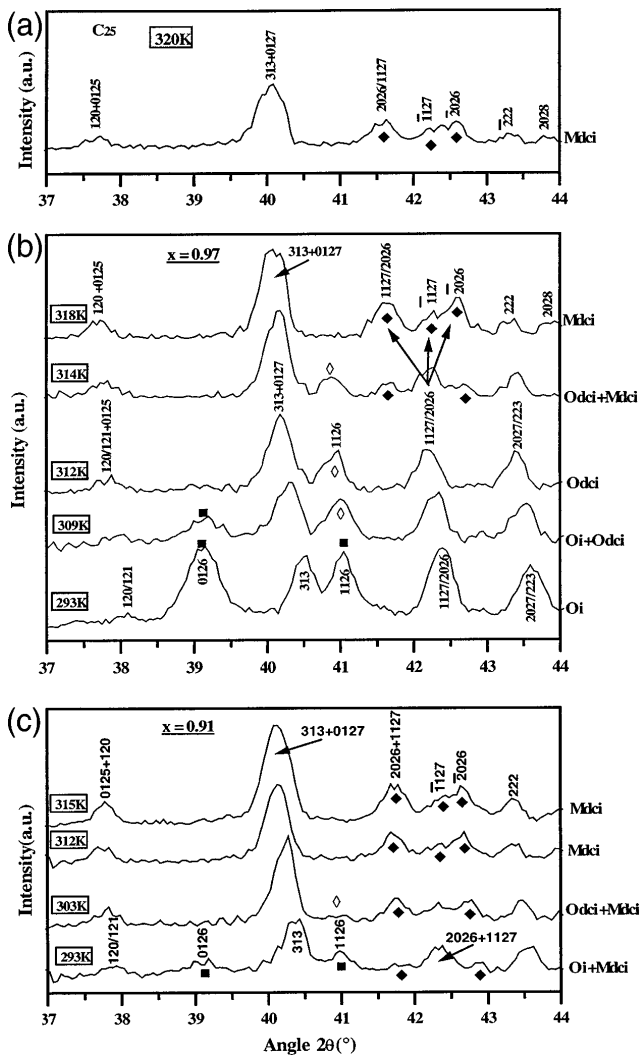


FIG. 3. System  $C_{23} + C_{25}$ : x-ray diffraction patterns of the low ordered phases in the range  $37^\circ \leq 2\theta \leq 44^\circ$  for (a)  $C_{25}$  at  $T = 320$  K, (b)  $x = 0.97$  at  $T = 293, 309, 312, 314,$  and  $318$  K, and (c)  $x = 0.91$  at  $293, 303, 312,$  and  $315$  K.

$O_{dci}$  transition [see Fig. 3(b)] is mainly characterized by the disappearance of the  $0\ 1\ 26$  reflection at  $2\theta \approx 39^\circ$ , while the intensity of the peaks at  $2\theta \approx 38^\circ$  and  $2\theta \approx 40.5^\circ$  increase due to the superposition of the  $0\ 1\ 25$  and  $0\ 1\ 27$  lines with the  $1\ 2\ 0/1\ 2\ 1$  and  $3\ 1\ 3$  reflections, respectively.

For  $x = 0.91$ , the sequence of domains is different [Fig. 3(c)]:  $[O_i + M_{dci}] \rightarrow [O_{dci} + M_{dci}] \rightarrow [M_{dci}]$ . The low-phase domains  $[O_i + M_{dci}]$  and  $[O_{dci} + M_{dci}]$  observed, respectively, at 293 and 303 K are clearly distinguished by the coexistence of two typical diffraction patterns. In the first case, the  $0\ 1\ 26$  reflection at  $2\theta \approx 39^\circ$  points out the existence of the phase  $O_i$  while the phase  $M_{dci}$  is characterized by the two weak diffraction lines due to the splitting of the reflections  $1\ 1\ 27$  and  $2\ 0\ 26$  at  $2\theta \approx 42.5^\circ$ . The disappearance

of the 0 1 26 reflection while the 1 1 26 line still persists (confirming the presence of the  $O_{dci}$  form) as well as the lines corresponding to the phase  $M_{dci}$  show the direct passage from  $[O_i + M_{dci}]$  to  $[O_{dci} + M_{dci}]$ , and, therefore, points out the existence of a metatectoid invariant located at  $T = (299 \pm 3)$  K, as shown in Fig. 2.

### C. The $M_{dci}$ form also exists in the molecular alloys rich in $C_{23}$

The structural behavior of the mixed sample  $x = 0.03$  with temperature in the low temperature region is chosen as an example. X-ray diffractograms recorded at  $T = 279, 293,$  and  $303$  K are shown in Fig. 4. It is clear forthright that the diffraction patterns represented in Fig. 3(a) at  $T = 320$  K, Fig. 3(b) at  $T = 318$  K, Fig. 3(c) at  $T = 315$  K, and Fig. 4 at  $T = 303$  K are very similar. This confirms the existence of two  $M_{dci}$  one-phase domains: one relatively close to  $C_{23}$  and the other one coming from  $C_{25}$ . Concerning the domain close to  $C_{23}$ , one can no more say that it is coming from the pure component, the  $M_{dci}$  phase of  $C_{23}$  being not a stable phase. The indexing of the diffraction lines both in the  $O_{dci}$  and  $M_{dci}$  forms in the mixed sample  $x = 0.03$  show something remarkable which has also been observed in the  $O_i$  form of the pure odd alkanes.<sup>39</sup> Comparing Fig. 3(a) ( $C_{25}$ ) and Fig. 4 ( $x = 0.03$ ) at  $T = 303$  K, we note that, for example, the lines in  $C_{25}$  and  $x = 0.03$  located at  $2\theta \approx 40^\circ$  is indexed as 0 1 27 and 0 1 25, respectively.

### D. Existence and nature of an $O_p$ phase in the central compositional region

Isotherm structural characterizations versus  $C_{25}$  molar concentration have been done both at 293 and 303 K. About twenty samples have been studied. As an example, we have chosen some characteristic patterns for  $T = 293$  K shown in Fig. 5. For clarity, the indexing of the reflections are not given in the figure. The x-ray

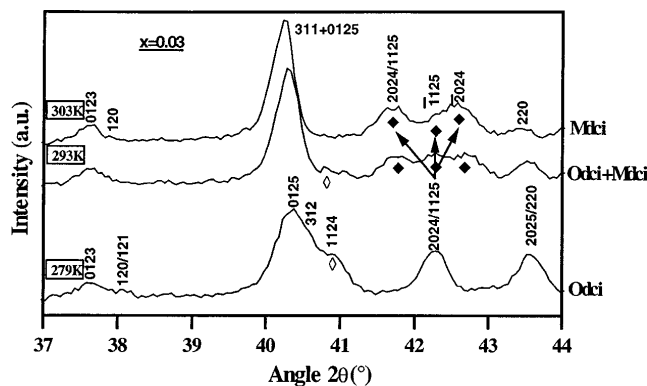


FIG. 4. System  $C_{23} + C_{25}$ : x-ray diffraction patterns of  $x = 0.03$  in the range  $37^\circ \leq 2\theta \leq 44^\circ$  at  $T = 279, 293,$  and  $303$  K.

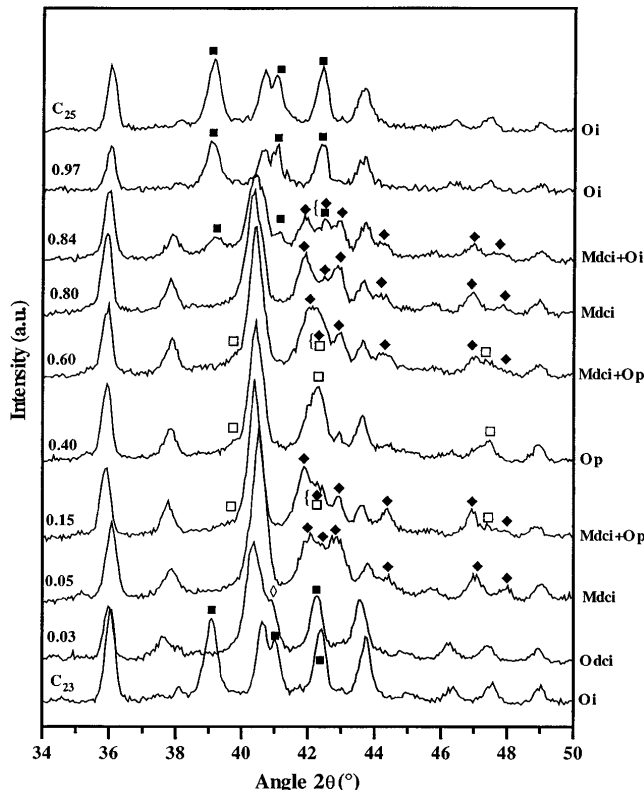
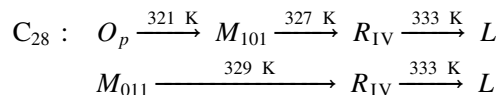


FIG. 5. System  $C_{23} + C_{25}$ : isothermal ( $T = 293$  K) structural characterizations versus  $C_{25}$  molar concentration in the range  $34^\circ \leq 2\theta \leq 50^\circ$ .

diffraction pattern of the sample  $x = 0.40$  is clearly different from those corresponding to the  $M_{dci}$  forms ( $x = 0.05$  and  $0.80$ ). It is, in fact, a new phase which is mainly characterized by the occurrence of reflections (symbolized by  $\square$ ) corresponding to  $2\theta \approx 39.5^\circ$ ,  $2\theta \approx 42.5^\circ$ , and  $2\theta \approx 47.2^\circ$ . We will discuss later the indexing of the diffraction lines in the  $O_p$  form. At  $T = 303$  K, the domain of this phase is a little wider than that at  $T = 293$  K (Fig. 2). What about the nature of the new phase we denote  $O_p$ ? To answer this question, the diffraction pattern of the alloy  $C_{23}$  ( $0.6$ )  $C_{25}$  ( $0.4$ ) is compared with that of the  $O_p$  form of octacosane ( $C_{28}$ ).

The polymorphic behavior of  $C_{28}$  is rather complex. Energetic and crystallographic analyses of  $C_{28}$ <sup>23</sup> (after melting and quenching) have shown that it crystallizes in two forms: monoclinic  $M_{011}$  (space group  $P_{21/a}$ ) and orthorhombic  $O_p$  (space group  $P_{ca2_1}$ ). The transition sequences observed with increasing temperature are the following:



Our purpose here is to show that the intermediate phase  $O_p$  observed in the binary system  $C_{23} + C_{25}$  is similar to the orthorhombic form of  $C_{28}$ . The diffraction

pattern of  $C_{28}$  (see Fig. 6) at 298 K shows the coexistence of the two forms ( $M_{011}$  and  $O_p$ ). However, we are interested in having the diffractogram of the orthorhombic phase alone. Smith<sup>30</sup> found that pure even alkanes above  $C_{26}$  normally crystallize as monoclinic at room temperature, but if impurities (neighboring homologues) exist, they crystallize in the orthorhombic form. We have thus prepared mixed samples of  $C_{28}$  with  $C_{26}$  molecules behaving like impurities (in fact, we have studied the binary system  $C_{26} + C_{28}$  which will be the subject, as said, in the introduction of another paper). Figure 6 also shows the diffraction patterns of some mixed samples  $C_{26} + C_{28}$  rich in  $C_{28}$ . We notice that the  $00l$  lines of the  $M_{011}$  form ( $\nabla$ ) diminish and finally disappear at the molar concentration of 0.85 in  $C_{28}$ . Hence, for this concentration, we obtain the diffractogram of the “pure” orthorhombic  $O_p$  form  $P_{ca2_1}$ . This diffractogram is given in Fig. 7(a) with the diffraction pattern of  $C_{23}$  (0.6)  $C_{25}$  (0.4) [Fig. 7(b)].

The “rule” for indexing the reflections of the odd alkanes in  $O_i$ ,  $O_{dci}$ , and  $M_{dci}$  forms and in mixed samples, cited previously, is also valid for the  $O_p$  forms. Indeed, independently of the number of carbon atoms [average  $C_{24}$  for  $C_{23}$  (0.6)  $C_{25}$  (0.4) and average  $C_{28}$  for  $C_{26}$  (0.18)  $C_{28}$  (0.85)], similar diffraction patterns are observed. For example, the peak at  $2\theta \approx 54^\circ$  correspond to the 3 1 25 reflection [see Fig. 7(b)] for  $C_{23}$  (0.6)  $C_{25}$  (0.4) and to the 3 1 29 reflection [Fig. 7(a)] for the  $C_{26}$  (0.15)  $C_{28}$  (0.85). The similarity of the two patterns allows us to say that the  $O_p$  forms observed are isomorphous. Therefore, the  $O_p$  form [Fig. 7(b)] observed in the  $C_{23}$ – $C_{25}$  system is also of space group  $P_{ca2_1}$ . More evidence for the space group  $P_{ca2_1}$  of the  $C_{23}$  (0.60)  $C_{25}$  (0.40) alloy is given by calculating its

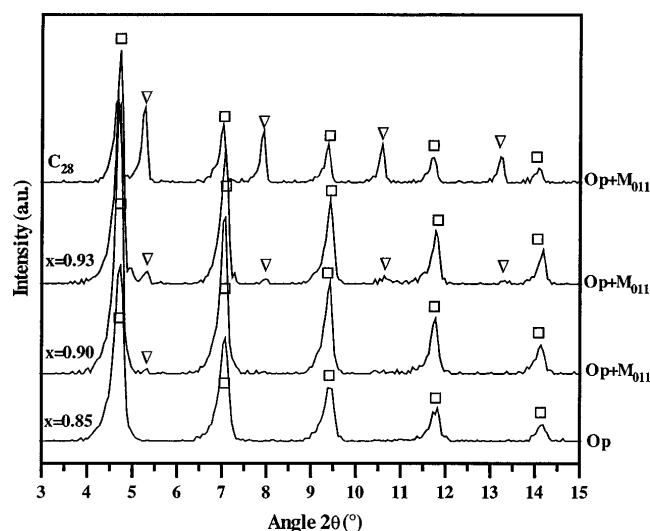


FIG. 6. X-ray diffractograms of  $C_{28}$  and of mixed samples  $x = 0.93$ ,  $0.90$ , and  $0.85$  in the range  $3^\circ \leq 2\theta \leq 15^\circ$  at  $T = 298$  K in the binary system  $C_{26}$ – $C_{28}$  ( $\nabla$ : symbol for  $M_{011}$ ).

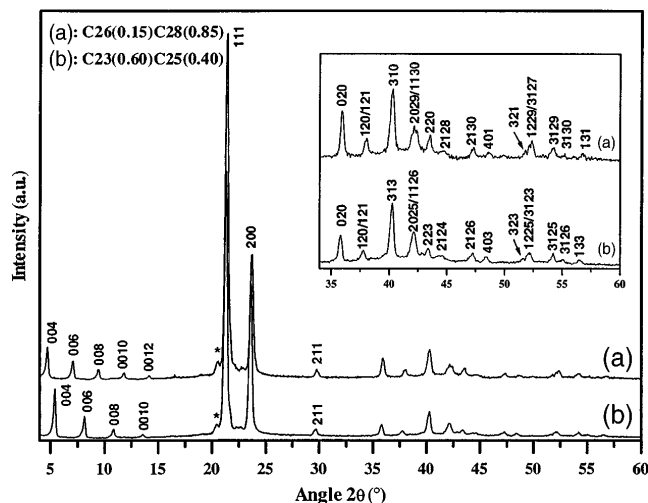


FIG. 7. Comparison between the diffractograms of the orthorhombic  $P_{ca2_1}$  form in the range  $4^\circ \leq 2\theta \leq 60^\circ$  (a) of the alloy  $C_{26}$  (0.15)  $C_{28}$  (0.85) and (b) of the  $O_p$  form of the alloy  $C_{23}$  (0.6)  $C_{25}$  (0.4).

theoretical diffraction pattern using the chain model proposed by Dorset.<sup>50,51</sup> The author gave the calculated fractional coordinates  $x/a$ ,  $y/b$ , and  $z/c$  of pure  $C_{30}$  in the  $P_{ca2_1}$  form. For our alloy, the calculation of the fractional coordinates given in Table I was done by assuming identical  $x/a$  and  $y/b$  coordinates ( $a$  and  $b$  cell parameters of the orthorhombic form of *n*-alkanes

TABLE I. Fractional coordinates of  $C_{23}$  (0.60)  $C_{25}$  (0.40) used to simulate the diffraction pattern by FULLPROF (hydrogen atoms are neglected and isotropic temperature for carbon atoms is  $B_c = 0.03$  nm<sup>2</sup>).

Atom	$x/a$	$y/b$	$z/c$	Occ.
$C_{(1)}$	0.014	0.186	0.0239	0.90
$C_{(2)}$	0.092	0.314	0.0435	1.00
$C_{(3)}$	0.014	0.186	0.0631	1.00
$C_{(4)}$	0.092	0.314	0.0827	1.00
$C_{(5)}$	0.014	0.186	0.1023	1.00
$C_{(6)}$	0.092	0.314	0.1219	1.00
$C_{(7)}$	0.014	0.186	0.1415	1.00
$C_{(8)}$	0.092	0.314	0.1611	1.00
$C_{(9)}$	0.014	0.186	0.1807	1.00
$C_{(10)}$	0.092	0.314	0.2003	1.00
$C_{(11)}$	0.014	0.186	0.2199	1.00
$C_{(12)}$	0.092	0.314	0.2395	1.00
$C_{(13)}$	0.014	0.186	0.2591	1.00
$C_{(14)}$	0.092	0.314	0.2788	1.00
$C_{(15)}$	0.014	0.186	0.2987	1.00
$C_{(16)}$	0.092	0.314	0.314	1.00
$C_{(17)}$	0.014	0.186	0.3376	1.00
$C_{(18)}$	0.092	0.314	0.314	1.00
$C_{(19)}$	0.014	0.186	0.3770	1.00
$C_{(20)}$	0.092	0.314	0.3964	1.00
$C_{(21)}$	0.014	0.186	0.4160	1.00
$C_{(22)}$	0.092	0.314	0.4356	1.00
$C_{(23)}$	0.014	0.186	0.4552	1.00
$C_{(24)}$	0.092	0.314	0.4748	0.90

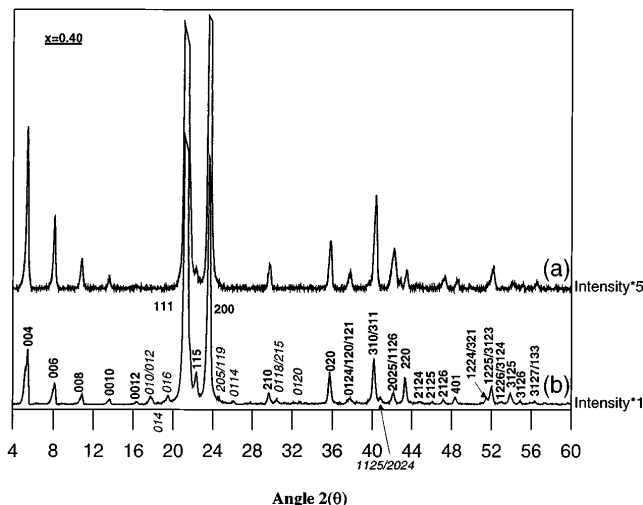


FIG. 8. X-ray diffraction pattern of the  $C_{23}$  (0.60)  $C_{25}$  (0.40) in the orthorhombic form  $P_{ca2_1}$  in the range  $4^\circ \leq 2\theta \leq 60^\circ$ : (a) experimental diffractogram and (b) simulated diffractogram using the FULLPROF program.

and binary mixed samples do not change significantly with chain length), and  $z/c$  coordinates were obtained by extrapolation along the  $z$ -axis of the chain model used by Dorset.<sup>51</sup> The fractional atomic occupancies (see Table I) which are applied to the chain ends have no effect on the angular position of the diffraction lines if not on the intensities and specially those of the  $00l$  lines. The fractional atomic occupancies are calculated only in order to satisfy the molar composition. The isotropic factors applied to carbon atoms ( $B_c = 0.03 \text{ nm}^2$ ) are those given by Dorset<sup>51</sup> and the effects of hydrogen atoms were neglected. The calculated diffractogram of the  $C_{23}$  (0.60)  $C_{25}$  (0.40) in the orthorhombic form was simulated using the “pattern-matching” option of the FULLPROF program<sup>52</sup> using the calculated fractional coordinates. Both experimental (a) and calculated (b) diffraction patterns of the  $C_{23}$  (0.60)  $C_{25}$  (0.40) are shown in Fig. 8 along with indexing corresponding to the lines with the strongest intensities and are very similar. Some calculated diffraction lines were not observed in the experimental diffractogram. Their absence is certainly due to preferential orientations.

### E. Cell parameter of the phases $O_p$ and $M_{dci}$

After a first refinement using the program AFMAIL, the final cell parameters were determined with the help of

the “Pattern-Matching” option of the FULLPROF program which allows, moreover, a comparison between the calculated and experimental diffractograms. The cell parameters of the mixed samples  $x = 0.05$ ,  $x = 0.40$ , and  $x = 0.80$  are given in Table II. For the  $M_{dci}$  forms, the cell parameters  $a$ ,  $b$ , and  $\beta$  are nearly the same as those of the  $M_{dci}$  form of  $C_{25}$ .

## VI. DISCUSSION AND CONCLUSION

X-ray diffraction analyses on the *n*-alkanes  $C_{23}$ ,  $C_{25}$ , and on the binary system  $C_{23} + C_{25}$  (with the help of the results on  $C_{26} + C_{28}$  binary system) have enabled us to reach a conclusion on the various phases observed at “low temperature” in the binary system  $C_{23} + C_{25}$ .

We have shown that the sequence of the one-phase domains with increasing  $x$  is the following:  $[O_i] \rightarrow [O_{dci}] \rightarrow [M_{dci}] \rightarrow [O_p] \rightarrow [M_{dci}] \rightarrow [O_{dci}] \rightarrow [O_i]$ . Thus, in contrast to the Jouti *et al.* conclusions,<sup>34,35</sup> all the molecular alloys are not orthorhombic: their  $\beta''1$  and  $\beta''2$  alloys are indeed both monoclinic  $M_{dci}$  ( $Aa$ ,  $Z = 4$ ).

On the other hand, the similarity of the diffraction patterns of the orthorhombic phase ( $P_{ca2_1}$ ,  $Z = 4$ ) of  $C_{26}$  (0.15)  $C_{28}$  (0.85) and of mixed samples of  $C_{23} + C_{25}$  near the equimolar composition has enabled us to state that the intermediate  $O_p$  form is  $P_{ca2_1}$  with four molecules per unit cell. This result is enhanced by the comparison between experimental and calculated diffractograms. At a first glance, it is quite surprising to see such a rich sequence of one-phase domains at low temperature despite the facts that the two components exhibit the  $O_i$  form on a very large temperature scale (until  $T = 310.5 \text{ K}$  for  $C_{23}$  and  $C_{25}$ <sup>1,22</sup>) and that their degree of crystalline isomorphism<sup>53</sup> is very high [ $\epsilon_m^i(O_i) = 0.92$ ]. We could expect *a priori* a very important miscibility not to say complete in the  $O_i$  form. Then, why do so many domains exist? The answer needs only one word: defects. Even if it is the same kind of defects (end-gauche ones) that is responsible for the observation of so many domains, the origin of these end-gauche defects is, however, different. Three cases are to be considered.

### A. The only (thermal) intrinsic defects

We consider the case of defects in the components themselves. It is known that in the shortest odd alkanes and in the low temperature  $O_i$  phase, the chains adopt an overall transconfiguration.<sup>54,55</sup> But we also

TABLE II. Cell parameters of the alloys in  $M_{dci}$  ( $Aa$ ,  $Z = 4$ ) and  $O_p$  ( $P_{ca2_1}$ ,  $Z = 4$ ) forms in the system  $C_{23} + C_{25}$ .

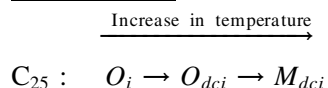
$x$ in $C_{25}$	$T$ (K)	Space group	Form	$a$ (nm)	$b$ (nm)	$c$ (nm)	$\beta$ ( $^\circ$ )
0.05	293	$Aa$	$M_{dci}$	0.749(0.2)	0.500(0.1)	6.263(0.4)	91.0(3)
0.40	298	$P_{ca2_1}$	$O_p$	0.753(0.2)	0.502(0.1)	6.511(0.3)	90
0.80	298	$Aa$	$M_{dci}$	0.753(0.1)	0.501(0.2)	6.734(0.5)	91.2(3)

know that those molecules are not absolutely rigid; conformational defects exist which are even more numerous and varied since the temperature and the chain length increase. These defects can be end-gauche, kink, double gauche, ... If the concentration of conformational defects is high, then the molecules can no more be considered as planar. We know that for both  $C_{23}$  and  $C_{25}$ , the defects which are concerned are mainly end-gauche ones found at the lamellar surface. As a result, a disruption of the packing of chain ends between molecular layers occurs which affects the interlamellar packing. The temperature increasing, the concentration of defects also increases and at a certain temperature, a jump in the concentration occurs (also accompanied by a jump in the interlayer spacing<sup>39</sup>), and a solid-solid transition takes place.<sup>9,56,57</sup> This is responsible for the polymorphism of the *n*-alkanes in the low temperature domain below the rotator phases. For example, in  $C_{25}$ , it explains the following solid-solid transitions:  $O_i \rightarrow O_{dci} \rightarrow M_{dci}$ . Recall that for  $C_{23}$ , the sequence is nearly the same but the  $M_{dci}$  form is not stable.

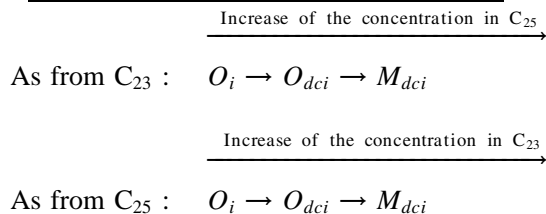
## B. The thermal and compositional defects

For the mixed samples, an increase in concentration of foreign molecules in the host crystal ( $C_{25}$  in  $C_{23}$  or  $C_{23}$  in  $C_{25}$ ) results (at a given temperature) in the same sequence (except that two-phase regions separating the one-phase regions are indeed observed). In other words, the increase of intrinsic defects ( $x = 0$  or 1, rise in temperature) and extrinsic defects (given temperature, rise in  $x$ ) result by the observation of the same sequence of solid ordered forms. This can be resumed by the following scheme:

Intrinsic defects:  $x = 0$  or 1; effect of the rise in temperature



Extrinsic defects: constant temperature; effect of the rise in concentration in foreign molecules



The extrinsic defects are essentially end-gauche defects,<sup>58,59</sup> i.e., as well as intrinsic (thermal) ones confined at the end of the chains. In other words, the additional effects of the thermal and compositional defects result

in the same transition sequences as for the pure components, but occurring at a lower temperature.

## C. What about the $O_p$ form?

The orthorhombic  $O_p$  form is observed in even alkanes as from  $C_{28}$ .<sup>6,7,23</sup> The crystal structure of this form was determined by Teare<sup>7</sup> on  $C_{36}$ . In fact, two forms were obtained, depending on the method of preparation: orthorhombic single crystals (space group  $P_{ca2_1}$ )<sup>7</sup> and monoclinic single crystals<sup>4</sup> (space group  $P_{2_1/a}$ ). Teare<sup>7</sup> noted that orthorhombic crystals were obtained from high-boiling petroleum ether solutions which contain paraffins up to hexane and probably higher members in solutions. This yields  $C_{36}$  crystals with impurities and could explain why an orthorhombic form was identified by Teare instead of the monoclinic form. These impurities would introduce conformational defects leading to the orthorhombic symmetry instead of the monoclinic one which is the more energetically stable (higher crystal density<sup>7</sup>). The orthorhombic  $O_p$  form is observed in the mixed samples of  $C_{23} + C_{25}$  near the equimolar composition. At the equimolar composition, the statistical molecular entity is very similar to the even alkane  $C_{24}$ . The result is that the end-gauche defects due to the geometrical mismatch caused by the two components of different chain length give rise to a different symmetry which is the orthorhombic form  $P_{ca2_1}$ ,  $Z = 4$  observed in higher even alkanes.

To our knowledge, only two works are found in the literature showing the molecular stacking in these three phases found in the pure components. Pieszczyk and co-workers,<sup>46,47</sup> studying *n*- $C_{33}$ , found four different phases denoted A, B, C (A =  $O_i$ , B =  $M_{dci}$  and C is monoclinic  $A_2$ ), and D the rotator phase which was defined later as the triclinic rotator phase  $R_{III}$ <sup>19,20</sup> which space group is still unknown. These authors suggested that the only possible motion which sets in with the phase transition A  $\rightarrow$  B ( $O_i \rightarrow M_{dci}$ ) is a chain rotation. In fact, we know that end-gauche defects were experimentally detected<sup>9</sup> at each phase transition ( $O_i \rightarrow O_{dci}$  and  $O_{dci} \rightarrow M_{dci}$ ) in  $C_{25}$ . Nozaki *et al.*<sup>21</sup> suggested that the end-gauche defects, even if they are in small amount, will introduce disorder in the layer surface, giving rise to different interlayer interaction and therefore to new molecular layer stacking. The solid ordered  $\rightarrow$  solid ordered phase transition in  $C_{23}$  and  $C_{25}$  are therefore characterized by changes in molecular layer stacking caused by the increased disorder in the layer surface. These authors give schematic projections along the molecular axes of the molecular layer stacking in each phase  $O_i$ ,  $O_{dci}$ , and  $M_{dci}$  (denoted by I, V, and IV, respectively) and reproduced in Figs. 9(a), 9(b), and 9(c) where only the carbon atoms are represented (solid circles indicate carbon atoms of the upper layer).

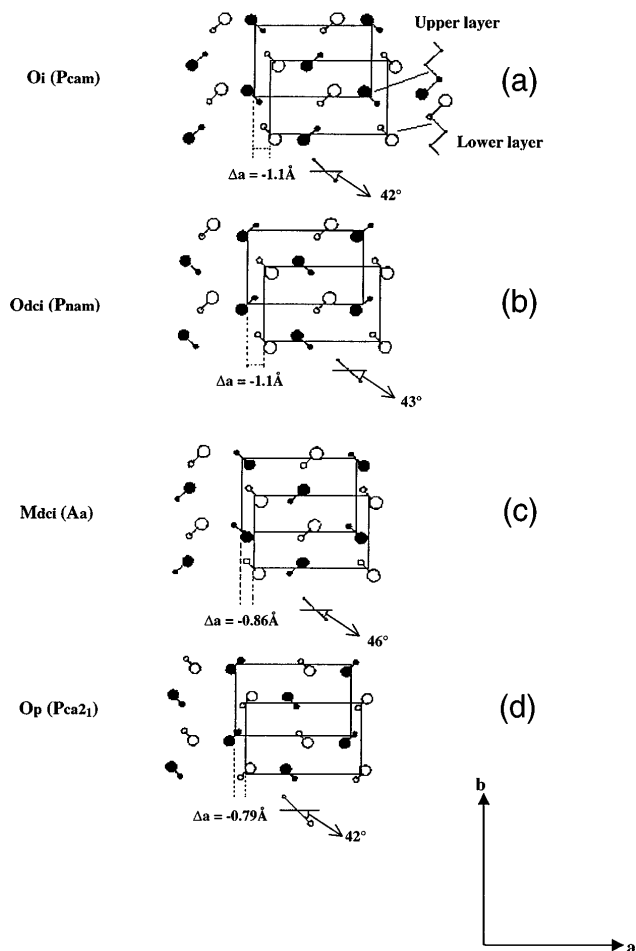


FIG. 9. Schematic projections along the molecular axes (*a*, *b*) of the molecular layer stacking in the phases  $O_i$ ,  $O_{dci}$ ,  $M_{dci}$ , and  $O_p$ . Only carbon atoms are represented. Solid circles represent carbon atoms in the upper layer and the hollow circles those in the lower layer.

In each of these phases, the molecules form a bilayer structure and it is convenient to use three parameters  $\Delta\phi$ ,  $\Delta a$ , and  $\Delta b$ <sup>46</sup> for expressing the bilayer structure.  $\Delta\phi$  is the rotation of the molecule about the chain axis in the upper layer relative to that of the lower layer, and the  $\Delta a$  and  $\Delta b$  are the shifts of the upper layer relative to the lower layer parallel to the *a*-axis and *b*-axis. In phase  $O_i$ , the layer stacking (upper layer with respect to the lower layer) is accompanied by a  $\Delta\phi = 180^\circ$  rotation of the molecules, the molecular shift parameters (shift of the upper layer to the lower layer) being  $\Delta a = -1.1 \text{ \AA}$  and  $\Delta b = b/2$ . In phase  $O_{dci}$ , the authors concluded a rotation of about  $90^\circ$  ( $\Delta\phi = 86^\circ$ ) [see Fig. 9(b)], while the molecular shift parameters remain almost the same. No molecular rotation occurs from  $O_{dci}$  to  $M_{dci}$  ( $\Delta\phi = 0^\circ$ ), while  $\Delta a = -0.86 \text{ \AA}$  [see Fig. 9(c)]. Let us note that the space groups used by these authors for the  $O_i$ ,  $O_{dci}$ , and  $M_{dci}$  forms are  $P_{bcm}$ ,  $P_{bnm}$ , and  $B_b$ , respectively. Interchanging parameters *a* and *b* yields the space groups  $P_{cam}$ ,  $P_{nam}$ , and  $Aa$  used in this

paper. The schematic projection along the molecular axes of the molecular layer stacking in the  $O_p$  phase in hexatriacontane  $C_{36}H_{74}$  is given in Fig. 9(d). The values of the three parameters are  $\Delta a = -0.79 \text{ \AA}$ ,  $\Delta b = b/2$ , and  $\Delta\phi = 180^\circ$ .

We note that only the layer stacking is different in the four phases; the side packing is orthorhombic and the molecules are perpendicular to the layer surface. Solid ordered  $\rightarrow$  solid ordered phase transitions in odd *n*-alkanes take place therefore by a restacking of the layers.<sup>21,48</sup> We suspect a similar behavior for the phases in the mixed samples as their cell parameters are quite the same (with the exception of the *c*-parameter which is a function of chain length). For example, starting from the  $C_{25}$  component, the phase sequence  $O_i \rightarrow O_{dci} \rightarrow M_{dci} \rightarrow O_p$  as a function of composition can be interpreted (for the  $O_i \rightarrow O_{dci} \rightarrow M_{dci}$ ) as for the  $C_{25}$  alkane as a function of temperature with possibly slight changes in the parameters  $\Delta a$ ,  $\Delta b$ , and  $\Delta\phi$ . The phase sequence  $M_{dci} \rightarrow O_p$  could be accompanied by a molecular rotation of  $\Delta\phi \approx 180^\circ$  with  $\Delta a \approx 0.21 \text{ \AA}$  and  $\Delta b \approx b/2$ . Further work is in progress for the experimental determination of the shift parameters by the Rietveld method using a structure model for mixed crystals.

This binary system is not the only one that has interested us. Indeed, we have performed a global study on binary systems of *n*-alkanes  $C_{n_1} + C_{n_2}$ ;  $n_1$  and  $n_2$  between 16 and 28, with  $\Delta n = 1$  or 2, with  $n_1$  and  $n_2$  both odd or even and also with  $n_1$  and  $n_2$  either odd and even or even and odd. The global synthesis of all these works is still in progress. Nevertheless, this synthesis is sufficiently advanced, enabling us to select the binary system  $C_{23} + C_{25}$  as the key system and, moreover, to state the number and the structural nature of the various forms of alloys. Indeed, we have pointed out that the  $O_p$  and the  $M_{dci}$  forms are also observed in many other binary systems of *n*-alkanes.

We are therefore able to say that this paper is widely beyond the scope of the only binary system presented here.

## REFERENCES

1. L. Roblès, D. Mondieig, Y. Haget, and M.A. Cuevas-Diarte, *J. Chim. Phys.* **95**, 92 (1998).
2. P. Espeau, L. Roblès, D. Mondieig, Y. Haget, M.A. Cuevas-Diarte, and H.A.J. Oonk, *J. Chim. Phys.* **93**, 1217 (1996).
3. A. Müller and M. Lonsdale, *Acta Crystallogr.* **1**, 129 (1948).
4. H.M.M Shearer and V. Vand, *Acta Crystallogr.* **9**, 379 (1956).
5. P.K. Sullivan and J.J. Weeks, *J. Res. NBS A* **74**, 203 (1970).
6. E.C. Reynhardt, J. Fenrych, and I. Basson, *J. Phys.: Condens. Matter* **6**, 7605 (1994).
7. P.W. Teare, *Acta Crystallogr.* **12**, 294 (1959).
8. M. Kobayashi, T. Kobayashi, Y. Ito, Y. Chatani, and H. Tadokoro, *J. Chem. Phys.* **72**, 2024 (1980).
9. R.G. Snyder, M. Maroncelli, S.P. Qi, and H.L. Strauss, *Science* **214**, 188 (1981).

10. Y. Urabe and K. Takamizawa, *Technology Reports of Kyusyu University* **67**, 85 (1994).
11. J. Doucet, I. Denicolo, and A. Craievich, *J. Chem. Phys.* **75** (3), 1523 (1981).
12. J. Doucet, I. Denicolo, A. Craievich, and A. Collet, *J. Chem. Phys.* **75** (10), 5125 (1981).
13. I. Denicolo, J. Doucet, and A. F. Craievich, *J. Chem. Phys.* **78** (3), 1465 (1983).
14. J. Doucet, I. Denicolo, A. F. Craievich, and C. Germain, *J. Chem. Phys.* **80** (4), 1647 (1984).
15. G. Ungar, *J. Phys. Chem.* **87**, 689 (1983).
16. M. Maroncelli, S. P. Qi, H. L. Strauss, and R. G. Snyder, *J. Am. Chem. Soc.* **104**, 6237 (1982).
17. S. P. Srivastava, J. Handoo, K. M. Agrawal, and G. C. Joshi, *J. Phys. Chem. Solids* **54** (6), 639 (1993).
18. S. R. Craig, G. P. Hastie, H. J. Roberts, and J. N. Sherwood, *J. Mater. Chem.* **4** (6), 977 (1994).
19. E. B. Sirota, H. E. King, Jr., D. M. Singer, and H. H. Shao, *J. Chem. Phys.* **98** (7), 5809 (1993).
20. E. B. Sirota, H. E. King, Jr., H. H. Shao, and D. M. Singer, *J. Phys. Chem.* **99**, 798 (1995).
21. K. Nozaki, N. Higashitani, T. Yamamoto, and T. Hara, *J. Chem. Phys.* **103** (13), 5762 (1995).
22. L. Roblès, European thesis of the University of Bordeaux I, France (1995).
23. B. Poirier, thesis of the University of Bordeaux I, France (1996).
24. F. Rajabalee, P. Espeau, and Y. Haget, *Mol. Cryst. Liq. Cryst.* **269**, 165 (1995).
25. P. Espeau, H. A. J. Oonk, P. R. van der Linde, X. Alcobe, and Y. Haget, *J. Chim. Phys.* **92**, 747 (1995).
26. L. Roblès, D. Mondieig, Y. Haget, M. A. Cuevas-Diarte, and X. Alcobe, *Mol. Cryst. Liq. Cryst.* **281**, 279 (1996).
27. L. Roblès, P. Espeau, D. Mondieig, Y. Haget, and H. A. J. Oonk, *Thermochim. Acta* **274**, 61 (1996).
28. H. Lüth, S. C. Nyburg, P. M. Robinson, and H. E. Scott, *Mol. Cryst. Liq. Cryst.* **27**, 337 (1974).
29. A. R. Gerson and S. C. Nyburg, *Acta Crystallogr.* **B50**, 252 (1994).
30. A. E. Smith, *Acta Crystallogr.* **10**, 802 (1957).
31. Z. Achour-Boudjema, J. B. Bourdet, D. Petitjean, and M. Dirand, *J. Mol. Struct.* **354**, 197 (1995).
32. Z. Achour, P. Barbillon, M. Bouroukba, and M. Dirand, *Thermochim. Acta* **204**, 187 (1992).
33. Z. Achour-Boudjema, M. Bouroukba, and M. Dirand, *Thermochim. Acta* **276**, 243 (1996).
34. B. Jouti, J. B. Bourdet, M. Bouroukba, and M. Dirand, *Mol. Cryst. Liq. Cryst.* **270**, 159 (1995).
35. B. Jouti, E. Provost, D. Petitjean, M. Bouroukba, and M. Dirand, *Mol. Cryst. Liq. Cryst.* **287**, 275 (1996).
36. H. Nouar, D. Petitjean, J. B. Bourdet, M. Bouroukba, and M. Dirand, *Thermochim. Acta* **293**, 87 (1997).
37. B. Jouti, E. Provost, D. Petitjean, M. Bouroukba, and M. Dirand, *J. Mol. Struct.* **382**, 49 (1996).
38. M. Dirand, Z. Achour, B. Jouti, A. Sabour, and J. C. Gachon, *Mol. Cryst. Liq. Cryst.* **275**, 293 (1996).
39. F. Rajabalee, European thesis of the University of Bordeaux I, France (1998).
40. V. Métivaud, F. Rajabalee, D. Mondieig, Y. Haget, and M. A. Cuevas-Diarte, *Chem. Mater.* (in press).
41. V. Métivaud, F. Rajabalee, M. A. Cuevas-Diarte, T. Calvet, D. Mondieig, and Y. Haget, *Anales de Quimica* (in press).
42. J. J. Retief, D. W. Engel, and E. G. Boonstra, *J. Appl. Crystallogr.* **18**, 156 (1985).
43. Y. Haget, R. Courchinoux, J. R. Housty, N. B. Chanh, M. A. Cuevas-Diarte, E. Tauler, T. Calvet, and E. Estop, *Calorim. Anal. Therm.* **XVIII**, 255 (1987).
44. R. Courchinoux, N. B. Chanh, Y. Haget, E. Tauler, and M. A. Cuevas-Diarte, *Thermochim. Acta* **128**, 45 (1988).
45. A. E. Smith, *J. Chem. Phys.* **21**, 2229 (1953).
46. W. Piesczek, G. R. Strobl, and K. Malzahn, *Acta Crystallogr.* **B30**, 1278 (1974).
47. B. Ewen, G. R. Strobl, and D. Richter, *Faraday Discuss. Chem. Soc.* **69**, 19 (1980).
48. K. Nozaki, T. Yamamoto, and M. Hikosaka, *J. Phys. Soc. Jpn.* **66** (11), 3333 (1997).
49. S. C. Nyburg and J. A. Potworowski, *Acta Crystallogr.* **B29**, 347 (1973).
50. D. L. Dorset, *Proc. Natl. Acad. Sci. U.S.A.* **87**, 8541 (1990).
51. D. L. Dorset, *Proc. Natl. Acad. Sci. U.S.A.* **30**, 451 (1997).
52. FULLPROF, a program for Rietveld refinement and pattern matching analyses, *Abstracts of the Satellite Meeting on Powder Diffraction of the XVth Congress of the International Union of Crystallography*, edited by J. Rodriguez-Carvajal, Toulouse, (1990), p. 127.
53. Y. Haget, L. Bonpunt, F. Michaud, P. Negrier, M. A. Cuevas-Diarte, and H. A. J. Oonk, *J. Appl. Crystallogr.* **23**, 492 (1990).
54. M. Maroncelli, S. P. Qi, H. L. Strauss, and R. G. Snyder, *J. Am. Chem. Soc.* **104**, 6237 (1982).
55. S. R. Graig, G. P. Hastie, and K. J. Roberts, *J. Mater. Sci.* **15**, 1193 (1996).
56. M. Maroncelli, S. P. Qi, H. L. Strauss, and R. G. Snyder, *J. Am. Chem. Soc.* **104**, 623 (1982).
57. Y. Kim, H. L. Strauss, and R. G. Snyder, *J. Am. Chem. Soc.* **93**, 7520 (1989).
58. M. Maroncelli, H. L. Strauss, and R. G. Snyder, *J. Phys. Chem.* **89**, 5260 (1985).
59. Y. Kim, H. L. Strauss, and R. G. Snyder, *J. Phys. Chem.* **93**, 485 (1989).